Rosen, J. M., Woo, S. L. C., & Comstock, J. P. (1975) *Biochemistry 14*, 2895.
Rosen, J. M., O'Neal, D. L., McHugh, J. E., & Comstock, J. P. (1978) *Biochemistry 17*, 290.
Spirin, A. (1963) *Prog. Nucleic Acids Res. 1*, 301.
Studier, F. W. (1965) *J. Mol. Biol. 11*, 373.
Towle, H. C., Dillman, W. H., & Oppenheimer, J. H. (1979) *J. Biol. Chem. 254*, 2250.
Tse, T. P. H., Morris, H. P., & Taylor, J. M. (1978) *Biochemistry 17*, 3121.
Wetmur, J. G., & Davidson, N. (1968) *J. Mol. Biol. 31*, 349.
Williams, J. G., Hoffman, R., & Penman, S. (1977) *Cell 11*, 901.
Wold, B. J., Klein, W. H., Hough-Evans, B. R., Britten, R. J., & Davidson, E. H. (1978) *Cell 14*, 941.
Woo, S. L. C., Rosen, J. M., Liarakos, C. D., Choi, Y. C., Means, A. R., O'Malley, B. W., & Robberson, D. L. (1975) *J. Biol. Chem. 250*, 7027.
Young, B. D., Birnie, G. D., & Paul, J. (1976) *Biochemistry 15*, 2823.

Internal Motions in Deoxyribonucleic Acid II†

Michael E. Hogan* and Oleg Jardetzky

ABSTRACT: We have measured the ^{1}H, ^{31}P, and ^{13}C NMR parameters of monodisperse deoxyribonucleic acid (DNA) fragments 260 and 140 base pairs long as a function of temperature and solvent viscosity. On the basis of these measurements, we calculate that within a rodlike DNA helix, the base planes, the deoxyribose sugar, and the sugar–phosphate backbone all experience large fast internal motions. The best fit of the data to a two-state model for internal motion specifies for the internal motions the following amplitudes A and correlation times τ: for the base planes, $A = \pm 20°$ and $\tau = 1 \times 10^{-9}$ s; for position 2′ of the deoxyribose sugar, $A = \pm 20$ to $\pm 33°$ and $\tau = 1 \times 10^{-9}$ s; for the P–H vectors of the sugar–phosphate backbone, $A = \pm 27°$ and $\tau = 2.2 \times 10^{-9}$ s.

In a recent study we measured the ^{31}P and ^{1}H NMR[1] parameters of short, monodisperse deoxyribonucleic acid (DNA) fragments. On the basis of that work, we were able to show that, in solution, a B DNA helix is not rigid but instead experiences fast fluctuations in the geometry of the deoxyribose sugar and of the phosphate–sugar backbone (Hogan & Jardetzky, 1979).

At that time, we modeled internal motion as being a fast two-state motion of H–H and P–H vectors relative to the long helix axis. Overall motion of the helix was treated as being that of a rod. In the context of that model, we calculated that in DNA the vector between adjacent methylene protons at deoxyribose position 2′ moves from its average geometry by ±35° with a time constant near 10^{-9} s. The three P–H vectors of the backbone phosphate were calculated to move by ±20° with a time constant also near 10^{-9} s.

We proposed that these motions could arise from a fluctuation of deoxyribose sugar pucker geometry, giving rise to a coupling of sugar and sugar–phosphate backbone motions. In small nucleotides, the conformations of the base and of the deoxyribose sugar are strongly coupled (Sundaralingam, 1975). Therefore, sugar-pucker fluctuations might be coupled to motions of the base planes in a B helix. Although narrow aromatic proton resonances could be measured in our previous study, indicating that they might be experiencing rapid internal motions, the complexity of aromatic proton relaxation made the unambiguous determination of that motion impossible.

Here, we present a detailed study of the effects of field strength, length, viscosity, and temperature upon the ^{31}P and ^{1}H relaxation properties of monodisperse fragments of B DNA. We show that the two-state model for internal motion in a rod fits well under all these experimental conditions and that under these conditions ^{31}P and ^{1}H relaxation is dominated by a simple dipolar relaxation mechanism. On the basis of these data, we calculate with greater accuracy the amplitude and time constant for internal motions in the helix. From the temperature dependence of these rates, we show that the activation energy for both phosphate and $H_{2'}$ proton motions is small, as expected for a true internal motion.

We also present, for the first time, ^{13}C NMR spectra and relaxation measurements made on a 260 base pair long DNA fragment. From measured T_1, NOE, and line-width values we show that deoxyribose sugar motions monitored by ^{13}C NMR are identical, within modeling accuracy, to the motions monitored by ^{1}H relaxation. We also show that, in addition to deoxyribose sugar motion, B DNA experiences a fast internal motion of base planes inside the helix which occurs with a time constant near 1×10^{-9} s.

Recently, Early and co-workers have obtained reasonably narrow, nearly length independent ^{1}H NMR spectra of the exchangeable aromatic H-bonded protons in long DNA helices (Early & Kearns, 1979). We have confirmed the observation with a monodisperse DNA fragment but show that proton dipolar relaxation contributes less to the line width of these protons than they have measured. Although amplitudes and time constants cannot be calculated from line widths alone, we propose that the small proton contribution to dipolar broadening of H-bonded resonances must be due to the large,

†From the Stanford Magnetic Resonance Laboratory, Stanford University, Stanford, California 94305. *Received February 1, 1980.* This research was supported by grants from the National Science Foundation (GP23633) and from the National Institutes of Health (RR00711). M.E.H. is a Fellow in Cancer Research supported by DR-6-283-F of the Damon Runyon–Walter Winchell Cancer Fund.

[1] Abbreviations used: DNA, deoxyribonucleic acid; NMR, nuclear magnetic resonance; NOE, nuclear Overhauser effect.

0006-2960/80/0419-3460$01.00/0

fast base-plane motion of the kind monitored by ^{13}C NMR.

Materials and Methods

The DNA fragments used in this work were prepared from calf thymus DNA (Sigma Chemical Co.). The DNA has been sonicated, digested with S1 nuclease, ribonuclease A, and protease K and then extracted with phenol and cold diethyl ether, as previously described (Hogan & Jardetzky, 1979). DNA was then fractionated by length on Sepharose 4B (Pharmacia).

DNA length was determined by electrophoresis on both native and denaturing polyacrylamide gels (Hogan & Jardetzky, 1979) relative to the *Hae*III restriction enzyme digest of ϕX174 (New England Biolabs). In all cases double-stranded and single-stranded DNA lengths were in agreement, indicating that the DNA used here is free from internal nicks or terminal single-stranded regions. The fragments were also digested analytically with S1 nuclease (Hogan & Jardetzky, 1979). The DNA fragments used for NMR measurements showed in all cases less than 2% S1 digestible material by this assay.

Two fractions with different lengths were used for ^{31}P and ^{1}H NMR measurements: S_{140}, average length 140 base pairs, length distribution ±20 base pairs; M_{260}, average length 260 base pairs, length distribution ±25 base pairs. The fragments used for ^{13}C NMR measurements were less monodisperse because of material requirements: average length 260 base pairs and length distribution ±40 base pairs. The distributions cited refer to that range of lengths which accounted for more than 75% of the DNA on gels.

Viscosity measurements have been made by using a capillary viscometer with temperature controlled to ±0.5 °C. In all cases, the measured values have been corrected for density changes.

Samples were prepared for NMR measurements by ethanol precipitation, followed by diaflow filtration and dialysis into the appropriate buffers. The DNA concentration was determined by using $\epsilon_{258} = 12\,900\ M^{-1}\ cm^{-1}$ (measured in base pairs). In those experiments which required sucrose, DNA samples were dialyzed against two changes of buffer containing analytical grade sucrose (Beckman) which had been previously dissolved in D_2O and lyophilized to remove exchangeable protons.

T_1 relaxation measurements have been made by using an inversion recovery pulse sequence. T_2 relaxation has been measured by using the Hahn spin-echo pulse sequence. NOE measurements have been made by comparing integrated areas of spectra accumulated with continuous broad-band proton decoupling to the areas accumulated with decoupling during the acquisition time only.

Fractional errors in T_1 and T_2 have been estimated from a linear least-squares fitting of the data and are calculated from twice the standard deviation from the mean. Fractional errors cited for line width and NOE measurements are calculated from the average deviation from the mean value of several experiments.

Theory

DNA fragments shorter than one persistence length behave hydrodynamically very much like rods (Hogan et al., 1978). The correlation time τ_L for rotational motion of the long axis of a rod is described by the Broersma relation (Broersma, 1960)

$$\tau_L^{-1} = \frac{18kT}{\pi\eta L^3}\left[\ln\frac{L}{b} - 1.57 + 7\left(\frac{1}{\ln(L/b)}\right) - 0.28^2\right] \quad (1)$$

where L is the length of the helix, b its width, and η the solvent viscosity. DNA fragments up to 200 base pairs long have been shown to obey this relationship rigorously (Hogan et al., 1978); fragments between 150 and 270 base pairs show deviations from rodlike behavior of less than 20% (Hogan et al., 1978; Kovacic & van Holde, 1977). For 140 base pair long DNA, eq 1 specifies $\tau_L = 3 \times 10^{-6}$ s, a value very near that measured for 140 base pair long DNA (Hogan et al., 1978). At 23 °C, eq 1 specifies $\tau_L = 1.3 \times 10^{-5}$ s for a 260 base pair long fragment. The value τ_L measured for 260 base pair long DNA is closer to 1.0×10^{-5} s, due presumably to small deviations from rodlike behavior (Hogan et al., 1978). Therefore, in our calculations we assume $\tau_{L,140} = 3 \times 10^{-6}$ s and $\tau_{L,260} = 1 \times 10^{-5}$ s.

The "speedometer cable" motion of the short axis of the helix must occur in rodlike DNA fragments but has never been accurately measured. The correlation time τ_S for this motion in a cylinder of length $2L$ is (Lamb, 1945; Barkley & Zimm, 1979)

$$\tau_S^{-1} = \frac{6kT}{8\pi\eta b^2 L} \quad (2)$$

For a 140 base pair long cylinder at 23 °C $\tau_S = 0.5 \times 10^{-7}$ s; for a 260 base pair long cylinder $\tau_S = 1 \times 10^{-7}$ s. We use these values in our calculations of the internal motion in 140 and 260 base pair long helices.

For long rods or ellipsoids which experience a single internal motion with correlation time τ_{int} which is much faster than τ_L or τ_S, the NOE and the relaxation rates T_1^{-1} and T_2^{-1} can be expressed as a linear sum of internal and overall motions (King & Jardetzky, 1978)

$$\frac{1}{T_2(\text{obsd})} = \frac{\alpha}{T_2(\tau_L)} + \frac{1-(\alpha+\beta)}{T_2(\tau_S)} \quad (3)$$

$$\frac{1}{T_1(\text{obsd})} = \frac{1-(\alpha+\beta)}{T_1(\tau_S)} + \frac{\beta}{T_1(\tau_{int})} \quad (4)$$

$$\frac{\text{NOE}-1}{\gamma_I/\gamma_S} \geq \frac{1-(\alpha+\beta)\phi(\tau_S)+\beta\phi(\tau_{int})}{1-(\alpha+\beta)\chi(\tau_S)+\beta\chi(\tau_{int})} \quad (5)$$

where the individual values $T_1(\tau)$, $T_2(\tau)$, $\phi(\tau)$, and $\chi(\tau)$ refer to expressions calculated for a single correlation time τ; γ_I and γ_S are respectively the gyromagnetic ratio of the observed nucleus and the nucleus to which it is dipolar coupled. α and β are coefficients which describe the relative contribution of τ_L and τ_{int} to NMR relaxation and are determined exclusively from molecular geometry (King & Jardetzky, 1978). Since the sum of these coefficients is normalized to 1 (King & Jardetzky, 1978), the coefficient corresponding to τ_S is expressed as $1-(\alpha+\beta)$.

For dipolar relaxation between protons at a distance r (Woessner, 1962)

$$\frac{1}{T_1(\tau)} = \frac{9}{8}\gamma_H^4\hbar^2 r^{-6}\left(\frac{4}{15}\frac{\tau}{1+(\omega_H^2)(\tau)^2} + \frac{16}{15}\frac{\tau}{1+4(\omega_H^2)(\tau)^2}\right) \quad (6)$$

$$\frac{1}{T_2(\tau)} = \frac{9}{40}\gamma_H^4\hbar^2 r^{-6} \text{ if } \tau \geq 5 \times 10^{-8}\text{ s} \quad (7)$$

where γ_H and ω_H are respectively the gyromagnetic ratio and Larmor frequency of protons in radians per second.

Table I: Length and Viscosity Dependence of ^{31}P NMR Relaxation

sample[a]	τ_L[c] (s^{-1})	τ_S (s^{-1})	T_1 (obsd)[d] (s)	T_1 (calcd)[e] (s)	NOE (obsd)	NOE (calcd)	T_2 (obsd) (ms^{-1})	T_2 (calcd) (ms^{-1})	$\Delta\nu_{1/2}$ (obsd) (Hz)	$\Delta\nu_{1/2}$ (calcd) (Hz)
S_{140}	3.0×10^{-6}	0.5×10^{-7}	3.2	3.35	1.35	1.35	32	36	22	9
M_{260}	1.0×10^{-5}	1.0×10^{-7}	3.6	3.6	1.37	1.37	13	12.5	39	25
M_{260} (30% sucrose; $\eta/\eta_0 = 2.6$[b])	2.6×10^{-5}	2.6×10^{-7}	3.9	3.8	1.40	1.38	4.2	4.8	76	66
M_{260} (60% sucrose; $\eta/\eta_0 = 5.2$)	5.2×10^{-7}	5.2×10^{-7}	3.8	3.8	1.41	1.39	3.1	2.4	120	133

[a] Sample conditions for M_{260} are as listed in the legend to Figure 1. S_{140} is in the same buffer, also at 23 °C. S_{140} concentration is equal to 4.2 mM in base pairs. [b] Viscosities listed for M_{260} have been measured at 23 °C with a capillary viscometer as described under Materials and Methods. Values are listed normalized to the viscosity in the absence of sucrose. [c] τ_L and τ_S have been calculated from the values at 23 °C in the absence of sucrose by assuming that they follow the viscosity dependence specified by eq 1 and 2 (see Theory). [d] T_1(obsd), T_2(obsd), NOE(obsd), and $\Delta\nu_{1/2}$(obsd) refer to experimentally determined values. Errors in T_1, NOE, T_2, and $\Delta\nu_{1/2}$ are estimated to be 5%, 5%, 20%, and 1 Hz, respectively. Errors have been estimated as described under Materials and Methods. [e] T_1, T_2, NOE, and $\Delta\nu_{1/2}$ values have been calculated from eq 3-11 (see Theory) by using the appropriate values for τ_L and τ_S and $\alpha = 0.065$, $\beta = 0.5$, and $\tau_{int} = 2.2 \times 10^{-9}$ s (see the text for details).

For ^{13}C proton or ^{31}P proton NMR relaxation (Doddrell et al., 1972)

$$\frac{1}{T_1(\tau)} = \frac{\hbar^2\gamma_{c,p}^2\gamma_H^2}{10} r^{-6}\chi(\tau) \quad (8)$$

$$\frac{1}{T_2(\tau)} = \frac{\hbar^2\gamma_{c,p}^2\gamma_H^2}{5} r^{-6}\tau \text{ if } \tau \geq 5 \times 10^{-8} \text{ s} \quad (9)$$

$$\chi(\tau) = \frac{\tau}{1 + (\omega_H - \omega_{c,p})^2(\tau)^2} + \frac{3\tau}{1 + (\omega_{c,p})^2(\tau)^2} + \frac{6\tau}{1 + (\omega_H + \omega_{c,p})^2(\tau)^2} \quad (10)$$

$$\phi(\tau) = \frac{6\tau}{1 + (\omega_H + \omega_{c,p})^2(\tau)^2} - \frac{\tau}{1 + (\omega_H - \omega_{c,p})^2(\tau)^2} \quad (11)$$

It is important to note that up to this step, no assumption has been made concerning the kind of internal motion which occurs; we assume only that it is independent of and faster than the overall motion of the helix and that the motion may be described by one correlation time. A particular model is necessary only to interpret the coefficients α and β in terms of angular fluctuations.

If a 140 base pair long helix were rigid, the slow motion of the long helix axis would give rise to ^1H, ^{13}C, or ^{31}P lines several kilohertz wide; the motion of the short helix axis is much faster and makes a much smaller contribution to the line widths. NMR spectra can be measured in long rodlike DNA helices *only* if a large, fast internal motion occurs relative to the long axis; motions relative to the short axis will have a much smaller effect. Therefore, we consider only internal motions relative to the long helix axis, modeling internal motion as a two-state fluctuation of relaxation vectors **r**(H–H,C–H,P–H) between the two angles θ_1 and θ_2 defined by **r** and the long helix axis. Using this model, we calculate (King et al., 1978)

$$\alpha = \frac{1}{16}(1 + 3\cos^2\bar{\theta}\cos\Delta) \quad (12)$$

$$\beta = \frac{3}{4}\sin^2\Delta \quad (13)$$

Here, $\bar{\theta} = (\theta_1 + \theta_2)/2$ is an average orientation of **r** with respect to the long axis, and $\Delta = \theta_1 - \theta_2$ is the amplitude of the two-state fluctuation.

The relaxation properties of long rods with an internal motion have several features which facilitate modeling. In these experiments τ_L and τ_S can be fixed independently by using monodisperse rodlike DNA fragments of defined length, so only α, β, and τ_{int} remain as variables in the relaxation equations for any fragment. For a true internal motion, α, β, and τ_{int} will not vary with changes in the overall correlation times. Therefore, the relaxation equations may be solved uniquely if T_1 and T_2 or the NOE and T_2 are measured for DNA fragments with different known values τ_L and τ_S.

The NOE is a particularly useful tool for evaluating internal motions in long rods. For rods longer than 140 base pairs ($\tau_S \geq 0.5 \times 10^{-7}$ s) the P{H} or C{H} NOE will be larger than its theoretical minimum only if the helix experiences large internal motions with a time constant faster than 10^{-7} s (Doddrell et al., 1972); the existence of a large NOE is, in fact, unambiguous proof of a fast motion. In addition, eq 5–11 predict that, if τ_S is increased, then the NOE should *increase* toward a limiting value which is expected to occur when τ_S approaches 10^{-6} s. At that limiting value, the NOE is a function of τ_{int} only. As τ_S approaches 10^{-6} s, the measured T_1 relaxation time also reaches a limiting value and is then a function of only β and τ_{int} independently.

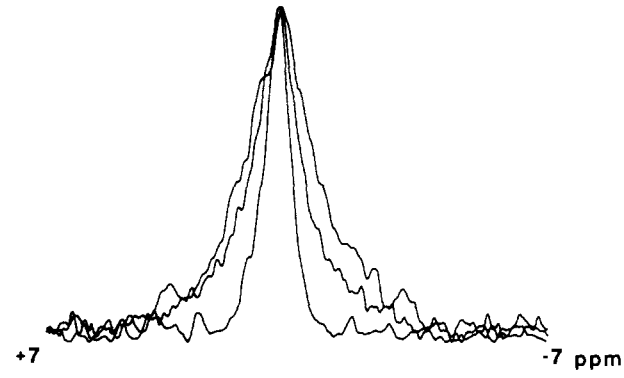

FIGURE 1: Effect of viscosity on the ^{31}P NMR line widths of 260 base pair long DNA. Samples have been dialyzed into 30 mM Tris, 3 mM Na_2EDTA, pH 7.3, and D_2O to which had been added the appropriate amounts of sucrose (see Materials and Methods). The DNA concentration was in all cases 4.8 mM, measured in base pairs. Fourier transform spectra have been accumulated at 40.511 MHz on a modified Varian XL 100 spectrometer equipped with a Varian multiple nuclei accessory. Spectra were accumulated with nonselective proton decoupling by using at all times a 90° Fourier pulse and a delay between pulses equal to 5 times the measured T_1 relaxation time. Chemical shifts are referenced to an external standard (85% H_3PO_4/15% D_2O). The temperature was controlled at +23 °C. Spectra have been presented with peak amplitudes normalized to the same value, so that line-width changes can be more easily compared. (Top) 40% sucrose, 1000 transients; (middle) 30% sucrose, 750 transients; (bottom) 0% sucrose, 500 transients.

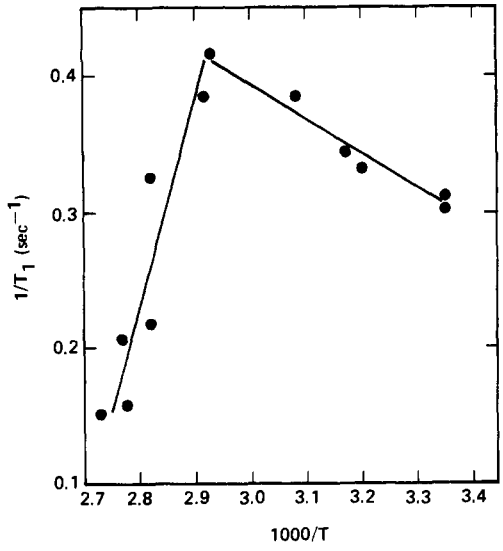

FIGURE 2: Effect of temperature on the ^{31}P T_1 relaxation time of 140 base pair long DNA. T_1 relaxation times were measured with continuous proton decoupling at 40.511 MHz by using an inversion recovery pulse sequence. The temperature was controlled to within 1 °C. Samples are in 20 mM Tris, 3 mM Na_2EDTA, pH 7.3, and D_2O. The DNA concentration was in all cases 3.0 mM, although no individual sample was used for more than three measurements. Upon completion of these measurements, DNA samples were run on denaturing polyacrylamide gels (see Materials and Methods) where they showed in all cases mobilities indentical with those prior to heating. Data are plotted as the T_1 relaxation rate $1/T_1$ in s^{-1} vs. the inverse of the temperature in kelvins.

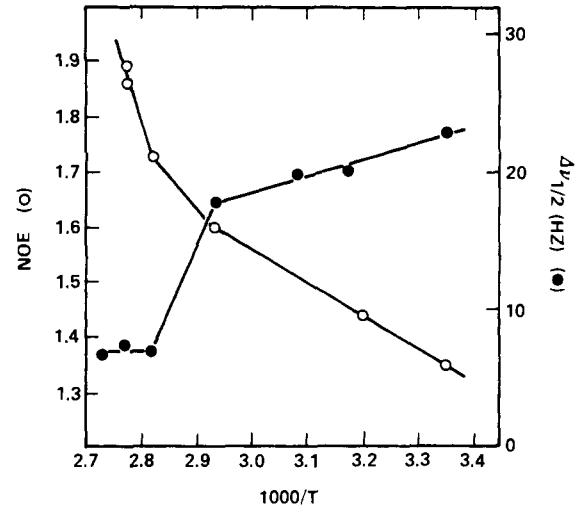

FIGURE 3: Effect of temperature on ^{31}P line widths and NOE values of 140 base pair long DNA. Sample conditions are as listed in Figure 2. ^{31}P NOE values have been measured by comparing the integrated area of spectra accumulated with continuous proton decoupling to that accumulated with the decoupler on during acquisition only. In all cases a 90° Fourier pulse was used with a delay between pulses equal to 5 times the measured T_1 relaxation time. (O) NOE values; (●) line widths $\Delta\nu_{1/2}$ (measured in Hz).

Results and Discussion

^{31}P NMR Measurements. We have measured the $^{31}P\{^1H\}$ NOE and the T_1 and T_2 relaxation times of 140 and 260 base pair long DNA fragments (S_{140} and M_{260}) with the intent of calculating the values β and τ_{int}. We present those results in Table I and Figure 1. As can be seen in Table I, both S_{140} and M_{260} show a measurable NOE. The NOE value measured for M_{260} is significantly larger than that of S_{140}, as expected from the length dependence of the NOE (see Theory). We have also increased the viscosity of the medium and have measured the relaxation properties of M_{260}. As expected from eq 3–11, the measured NOE and T_1 values increase to a constant value, while T_2 decreases linearly with the viscosity.

These measurements suffice to calculate α, β, and τ_{int}. The best fit of eq 3–11 to the data specifies $\alpha = 0.065$, $\beta = 0.5$, and $\tau_{int} = 2.2 \times 10^{-9}$ s at 23 °C. These compare well with the less accurate values ($\beta = 0.60$ and $\tau_{int} = 1 \times 10^{-9}$ s) which we measured earlier (Hogan & Jardetzky, 1979). As can be seen in Table I, the agreement between the model and the data is good and independent of DNA fragment length or solvent viscosity. In making these calculations we have assumed only that ^{31}P relaxation occurs as the sum of three vectors, $P–H_{3'}$, $P–H_{5_1'}$, and $P–H_{5_2'}$, all with a separation $r = 2.8$ Å (Arnott et al., 1969). As can be seen in Table I, T_1 and NOE values calculated from the two-state model agree well with the measured values. Therefore, as has been noted elsewhere (Klevan et al., 1979), ^{31}P relaxation in DNA appears to be predominantly dipolar at 40.51 MHz.

In the context of the two-state model (eq 12 and 13), the calculated value β specifies $\Delta = 55°$; on the average, the three P–H vectors fluctuate from their averaged geometries by ±27° with a time constant near 2.2×10^{-9} s. We estimate that within the limits of the two-state model the amplitude and time constants calculated here are accurate to within 30%.

Rate theory predicts that if the motion monitored by ^{31}P NMR is a true internal motion, with a rate near 10^9 s^{-1}, then its activation energy should be near kT (0.6 kcal at 23 °C). To confirm this, we have measured the ^{31}P T_1 relaxation time, line width, and NOE at several temperatures, presenting that data in Figures 2 and 3 and in Table II. As seen, T_1 decreases by approximately 20% between 25 and 68 °C, while the NOE increases from 1.35 to 1.60. The T_1, NOE, and line width all show a sharp discontinuity at 68 °C, which is the temperature at which DNA melting begins at this ionic strength (Hogan & Jardetzky, 1979). Above the melting transition NOE increases sharply, while T_1 decreases, indicating that the slowest motions sampled by T_1 or NOE have become faster than 2×10^{-9} s, as expected if these fragments are behaving as random coils. Interestingly, at high temperature the measured NOE appears to be rapidly approaching its theoretical fast-motion limit (NOE = 2.25). Such large values can occur in DNA only if P–H relaxation is predominantly dipolar (Doddrell et al., 1972).

Below the helix melting transition, we have obtained a fit of the measured line-width, T_1, and NOE values of eq 3–11. For these calculations we have assumed that τ_S varies as specified by the measured bulk viscosity in eq 2; motion of the long helix axis has already been shown to increase with temperature as predicted from eq 1 (Hogan et al., 1978). From this, we calculate that the internal correlation time, τ_{int}, monitored at phosphate, decreases from 2.2×10^{-9} to 1.5×10^{-9} s between 25 and 60 °C, while β increases from 0.5 to 0.8 (Table II). In Figure 4 we present an Arrhenius plot of this rate data which specifies an apparent activation energy $E_{act} = 1.8$ kcal. This calculated energy represents an *upper limit* to the true activation energy. The values τ_{int} have been calculated by assuming rodlike behavior at all temperatures, yet it is known that the DNA persistence length is itself moderately temperature dependent (Gray & Hearst, 1968). Any increase in the flexibility of the helix would reduce the changes calculated for both β and τ_{int}, thereby reducing E_{act}. E_{act} is therefore small, as expected for a fast internal motion.

^1H NMR Measurements. We have measured the T_1 and T_2 relaxation times of M_{260} as a function of temperature and field strength, presenting the data in Figure 5 and Table III. As we have shown earlier (Hogan & Jardetzky, 1979), four well resolved resonance bands may be measured in DNA:

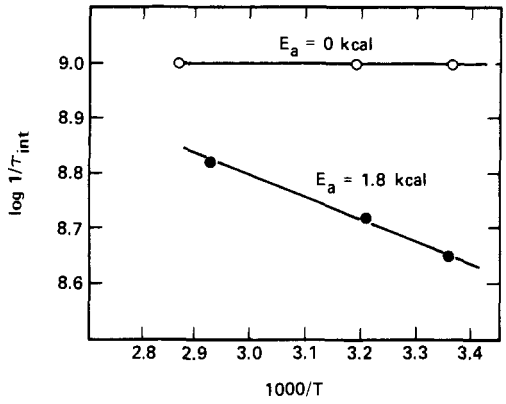

FIGURE 4: Arrhenius plot of internal correlation times calculated for $H_{2'}$ protons and for phosphate. The data presented are from Tables I and III and are plotted as the log of the inverse of the internal relaxation rate (log $1/\tau_{int}$) vs. the inverse of the temperature. (○) $H_{2'}$; (●) phosphate.

band I (H_2, H_6, and H_8), band II ($H_{1'}$ and H_5), band V ($H_{2'}$), and band VI (CH_3). As we have shown earlier and as can be seen in Figure 5b,c, the positions and areas of these bands are essentially unchanged over the entire range of temperatures below the helix melting transition. As seen in Figure 5a, upon melting of the helix (accomplished in this case by lowering the ionic strength to 20 mM at 75 °C), resonances move downfield and sharpen dramatically.

The relaxation times T_1 and T_2 of protons $H_{2'}$ in M_{260} are given in Table III. T_1 is insensitive to temperature below the melting transition although T_2 increases by more than a factor of 2. We have fit these data to the two-state model, calculating that the amplitude and correlation time of the internal motion monitored by $H_{2'}$ are both independent of temperature. Therefore, $E_{act} \simeq 0$, as expected for a true internal motion.

In our modeling we have assumed that $H_{2'}$ relaxation arises from a simple dipolar interaction between adjacent methylene protons (r = 1.78 Å). In large macromolecules, cross-relaxation effects (spin diffusion) could also contribute to $H_{2'}$ proton relaxation, although, in the presence of large fast $H_{2'}$–$H_{2'}$ motions, that contribution should be small (Kalk & Berendsen, 1976). To confirm that cross relaxation is not a contributing factor, we have measured proton T_1 values at 100 as well as at 360 MHz (Table III).

The cross-relaxation contribution to dipolar relaxation is sensitive to slow molecular motions and is expected in large macromolecules to be nearly field independent (Kalk & Berendsen, 1976). As can be seen in Table IV, the measured T_1 relaxation time is not field independent but instead decreases by a factor of 8 between 360 and 100 MHz. A simple H–H dipolar interaction can account for this decrease alone (Table III), suggesting that spin diffusion does not contribute significantly to T_1 relaxation of $H_{2'}$ protons.

As seen in Table III, the best fit of T_1 and T_2 relaxation times to eq 3–11 specifies β = 0.64 and $\tau_{int} = 1.0 \times 10^{-9}$ s (as compared to the less accurate values β = 0.66 and $\tau_{int} = 4 \times 10^{-9}$ s, which we calculated earlier). In the context of the two-state model this solution suggests that the $H_{2'}$–$H_{2'}$ vector experiences a ±33° fluctuation in the helix with a time constant near 1.0×10^{-9} s. Errors in these two values are estimated to be near 30%.

^{13}C NMR Measurements. The ^{13}C T_1, NOE, and line-width values for M_{260} are shown in Figure 6 and Table IV. As seen in Figure 6, we can measure the spectra of both aromatic and deoxyribose carbons in the helix. On the basis of NMR studies of the individual nucleotides (Dorman & Roberts, 1970; Jones et al., 1970), we make the following tentative assignments:

Table II: Temperature Dependence of ^{31}P NMR Relaxation for 140 Base Pair Long DNA[a]

temp (°C)	η/η_{25}[b]	τ_L[c] (s)	τ_S[c] (s)	τ_{int}[d] (s)	α[d]	β[d]	T_1(obsd)[e] (s)	T_1(calcd)[f] (s)	NOE(obsd)[e]	NOE(calcd)[f]	ΔW (obsd)[e]	ΔW (calcd)[f]
23	1	3.0×10^{-6}	0.50×10^{-7}	2.2×10^{-9}	0.065	0.5	3.2	3.2	1.35	1.35	0	0
39	0.72	2.2×10^{-6}	0.36×10^{-7}	1.9×10^{-9}	0.065	0.6	3.0	3.0	1.44	1.44	3	2
68	0.45	1.4×10^{-6}	0.25×10^{-7}	1.5×10^{-9}	0.065	0.8	2.5	2.5	1.60	1.60	5	4.5

[a] Sample conditions are as listed in Figure 2. [b] Sample viscosities listed have been measured experimentally as described under Materials and Methods and are listed relative to the value measured at 25 °C. [c] τ_L and τ_S values have been calculated from the values at 25 °C by using measured viscosities and eq 1 and 2 (see Theory). [d] τ_{int}, α, and β have been calculated from the model described under Theory. [e] Errors in observed values of T_1, NOE, and ΔW are calculated to be 5%, 5%, and 1 Hz, respectively. Errors are calculated as described under Materials and Methods. ΔW refers to the change in line width relative to 25 °C. [f] The T_1, NOE, and ΔW values expected from the motional model [T_1(calcd), NOE(calcd), and ΔW(calcd)] are presented for comparison with the data.

Table III: Temperature Dependence of ^1H NMR Relaxation for 260 Base Pair Long DNA[a]

temp (°C)	η/η_{25}[b]	τ_L[c] (s)	τ_S[c] (s)	τ_{int}[d] (s)	α[d]	β[d]	T_1 (obsd)[e] (s)	T_1 (calcd)[f] (s)	T_2 (obsd) (ms)	T_2 (calcd) (ms)
25	1	1.0×10^{-5}	1.0×10^{-7}	1×10^{-9}	<0.05	0.64	1.0	0.91	3.5	3.8
25 (100 MHz)	1	1.0×10^{-5}	1.0×10^{-7}	1×10^{-9}	<0.05	0.64	0.13	0.14	5	3.8
40	0.73	0.7×10^{-5}	0.7×10^{-7}	1×10^{-9}	<0.05	0.64	1.1	0.90	5	5.4
75	0.40	0.4×10^{-5}	0.4×10^{-7}	1×10^{-9}	<0.05	0.64	1.1	0.90	8	9.4
75 (denatured)	0.40						0.39		15	

[a] Sample conditions are in all cases as described in Figure 5. Relaxation times at 100 MHz have been accumulated on a Varian XL 100 spectrometer. Other conditions for ^1H NMR accumulation at 100 MHz are as listed in Figure 5. [b] Sample viscosities have been measured as described under Materials and Methods and are listed relative to the value at 25 °C. [c] τ_L and τ_S values have been calculated from measured viscosities and eq 1 and 2 (see Theory). [d] τ_{int}, α, and β have been calculated from experimentally determined T_1 and T_2 values by using eq 3-11. [e] T_1 and T_2 have been measured as described under Materials and Methods. Errors in T_1 and T_2 are estimated to be 10 and 20%, respectively. [f] T_1 and T_2 have been calculated for purposes of comparison with the data (see the text for details).

Table IV: ^{13}C NMR Properties of 260 Base Pair Long DNA

peak	assignment	no. of protons	measd area[a]	predicted area	T_1 (obsd)[b] (s)	T_1 (calcd)[c] (s)	NOE (obsd)[b]	NOE (calcd)[c]	$\Delta\nu_{1/2}$ (obsd)[b] (Hz)	$\Delta\nu_{1/2}$ (calcd)[c] (Hz)
1	nonprotonated aromatic	0	3.2	2.5	0.25		1.2	1.15	290	
2	nonprotonated aromatic, C_2	0, 1			0.40		1.1	1.15	350	
3	C_6, C_8	1	0.95	1	0.13	0.15	1.9	2.1	110	≥95
4	C_5	0, 1	0.9	1	0.45		1.0		275	
5	$C_{1'}$, $C_{3'}$, $C_{4'}$, $C_{5'}$	1, 2	3.5	4	0.14	0.15	2.3	2.1	150	≥95
6	$C_{2'}$	2	1	1	0.08	0.08	1.9	2.1	220	≥190
7	CH_3	3	0.5	0.3	0.35		2.6		70	

[a] Areas have been measured from decoupled spectra without NOE. Areas are estimated to be accurate to within 20%. [b] Errors in T_1, NOE, and $\Delta\nu_{1/2}$ are estimated to be 20%, 25%, and 20 Hz, respectively (see Materials and Methods for a description of error determination). [c] T_1, NOE, and $\Delta\nu_{1/2}$ values have been calculated for peaks 3, 5, and 6 by using eq 3-11 (see Theory) and $\tau_L = 2 \times 10^{-5}$ s, $\tau_S = 1 \times 10^{-7}$ s, $\tau_{int} = 1 \times 10^{-9}$ s, $\alpha = 0$, and $\beta = 0.3$. See the text for additional details.

Table V: Line Widths of Exchangeable H-Bonded Resonances in 140 Base Pair Long DNA[a]

sample	$\Delta\nu_{1/2}$(AT)[b] (Hz)	$\Delta\nu_{1/2}$(GC) (Hz)
100% H_2O	275	212
30% H_2O	270	220

[a] Sample conditions are as described in Figure 7. [b] The values cited are the average of five independent measurements. Errors are estimated to be 5 Hz as described under Materials and Methods.

band 1, nonprotonated aromatics; band 2, C_2 of adenine and nonprotonated aromatics; band 3, protonated carbons C_6 and C_8; band 4, both protonated and nonprotonated carbons C_5; band 5, deoxyribose carbons $C_{1'}$, $C_{3'}$, $C_{4'}$, and $C_{5'}$; band 6, $C_{2'}$; band 7, CH_3. The downfield part of band 5 is likely to contain $C_{1'}$ and $C_{3'}$ carbons only. As seen in Table V, the relative areas measured for the seven bands are nearly as expected for calf thymus DNA, arguing that nearly every carbon of the base plane and of the deoxyribose sugar in DNA contributes to the spectrum. The signal intensity attainable in these measurements indicates that, as was seen in ^{31}P and ^1H NMR, nearly every base pair in the helix contributes to these spectra.

The measured NOE values of bands 3, 5, 6, and 7 are all large. The theoretical maximum value for C–H relaxation is 3.0 (Doddrell et al., 1972); therefore, the measured NOE values clearly show, without need for any assumption as to the nature of the motion, that the base plane carbons C_6 and C_8, the deoxyribose carbons $C_{1'}$–$C_{5'}$, and the thymidine methyl group all experience fast internal motion inside a 260 base pair long helix. As expected (Doddrell et al., 1972) those bands composed of nonprotonated carbons (1, 2, and 4) show no measurable NOE.

Also of interest in Table III are the exceedingly short T_1 relaxation times and narrow line widths which are measured for the protonated carbons in DNA (bands 3, 5, and 6). At 25.1 MHz, ^{13}C NMR relaxation of protonated carbons in nucleic acids is expected to be exclusively dipolar (Doddrell et al., 1972). If the helix were rigid, then ^{13}C T_1 values and line widths would be too large to measure. As was the case for the NOE, the small T_1 and line-width values measured for DNA show, again without assumption as to the nature of the motion, that the base planes and the deoxyribose sugar experience large fast motions inside the helix.

We have fit the relaxation data measured for protonated carbons in DNA to eq 3–11. The data and the corresponding fits are shown in Table IV. For purposes of calculation we have assumed $r = 1.1$ Å, $\tau_L = 1 \times 10^{-5}$ s, and $\tau_S = 1 \times 10^{-7}$ s. Within experimental accuracy, the data for both singly and doubly protonated carbons are well fit by $\beta = 0.3$ and $\tau_{int} = 1 \times 10^{-9}$ s (Table IV). In the context of the two-state model (eq 12 and 13), this specifies that the base planes at positions C_6 and C_8 and the deoxyribose carbons at $C_{1'}$, $C_{3'}$, and $C_{2'}$ all experience ±20° fluctuations in geometry which occur with a time constant near 1×10^{-9} s.

Exchangeable H-Bonded Resonances. Early and co-workers have shown that relatively narrow resonances may be measured for the aromatic nitrogen protons in AT and GC base pairs (Early & Kearns, 1979). We confirm this observation with the monodisperse fragment S_{140} and present its proton spectrum in Figure 7. The resonance at 13.5 ppm corresponds to N(3) protons of AT base pairs and that at 12.4 ppm to the N(1) protons of GC base pairs (Early & Kearns, 1979).

As Early and colleagues have correctly noted (Early & Kearns, 1979), H-bonded resonances can be this narrow only if the helix experiences fast internal motion. Therefore,

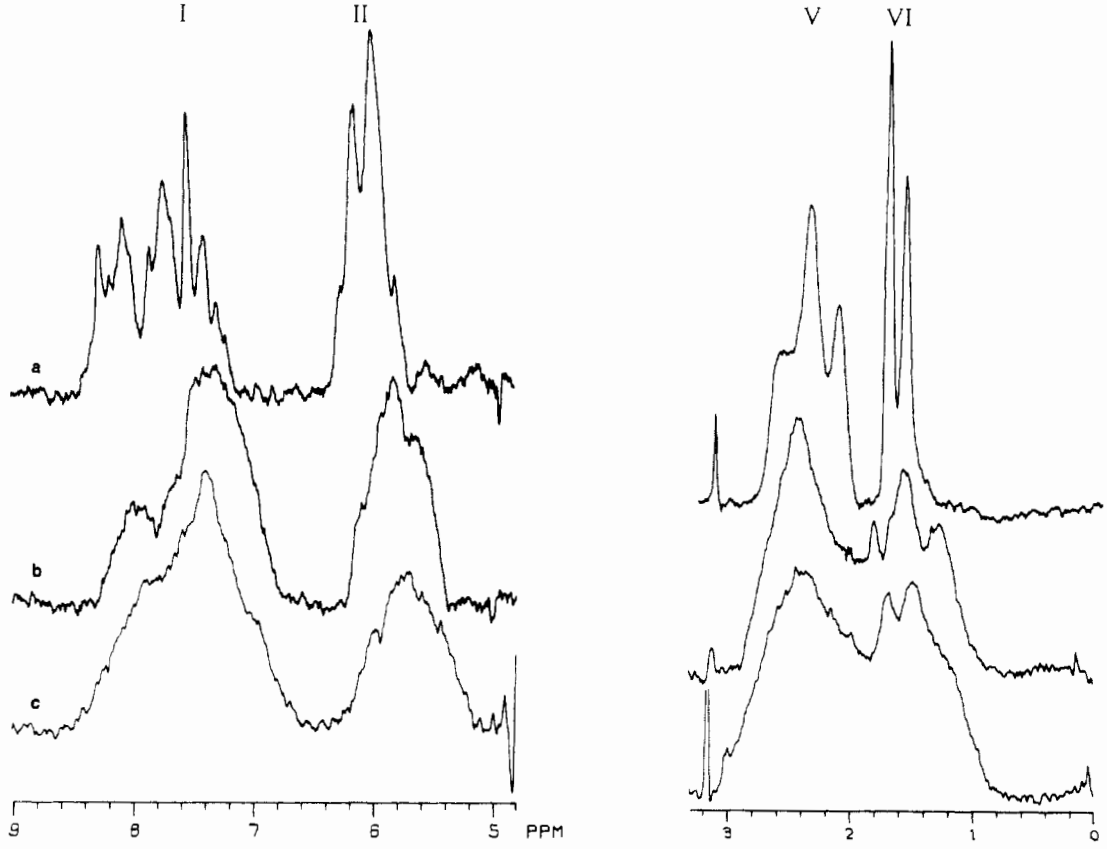

FIGURE 5: Effect of temperature on the ^1H NMR spectrum of 260 base pair long DNA. Fourier transform spectra were accumulated on a Bruker HXS-360 spectrometer using a 90° pulse and a delay between acquisitions equal to 5 times the longest measured T_1 relaxation time. Chemical shifts have been referenced relative to external Me_4Si. The DNA concentration is held constant and equal to 4.8 mM in base pairs. In all cases the spectra represent the average of 1000 transients. (a) (75 °C, denatured DNA) 20 mM NaCl, 6 mM Na_2HPO_4, 2 mM NaH_2PO_4, 1 mM Na_2EDTA, pH 7.2, and D_2O. (b) (75 °C, native DNA) 200 mM NaCl, 6 mM Na_2HPO_4, 2 mM NaH_2PO_4, 1 mM Na_2EDTA, pH 7.2, and D_2O. (c) (25 °C, native DNA) 200 mM NaCl, 6 mM Na_2HPO_4, 3 mM NaH_2PO_4, 1 mM Na_2EDTA, pH 7.2, and D_2O.

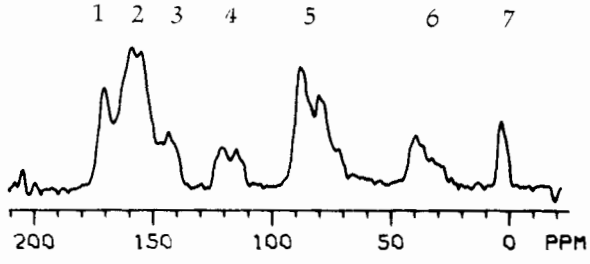

FIGURE 6: ^{13}C NMR spectrum of 260 base pair long DNA. M_{260} is in 200 mM NaCl, 6 mM Na_2HPO_4, 2 mM NaH_2PO_4, 1 mM Na_2EDTA, pH 7.2, and D_2O. The DNA concentration is 120 mM in base pairs. The temperature was held constant at 32 °C to reduce sample viscosity. The spectrum has been accumulated at 25.1 MHz on the Varian XL 100 spectrometer described in the legend to Figure 1 and represents the average of 36 000 transients. Measurements have been made by using a 90° pulse and a delay equal to 5 times the longest measured T_1 value of the spectrum. Proton decoupling has been performed during the acquisition time only. This spectrum therefore presents decoupled resonances without NOE so that areas may be compared directly. Upon completion of ^{13}C NMR measurements with M_{260}, double-stranded and single-stranded DNA lengths were re-measured on polyacrylamide gels and were found to be unchanged (see Materials and Methods).

without assumption, these narrowed line widths also confirm that the base planes in DNA experience fast, large amplitude motions.

A detailed interpretation of the motion is, however, more complicated. Early and Kearns have measured a substantial contribution to H-bonded proton line widths resulting from dipolar relaxation between protons within the base pair (Early & Kearns, 1979). On the basis of that value for the dipolar line width, they have modeled the motion which occurs in

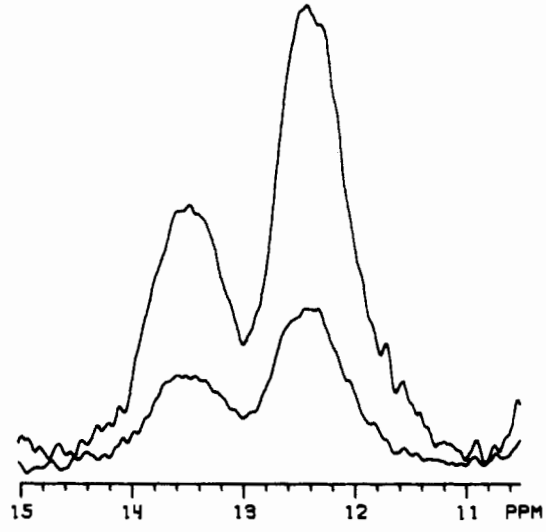

FIGURE 7: Effect of deuteration on H-bonded proton line widths of 140 base pair long DNA. Samples have been dialyzed into 200 mM NaCl, 6 mM Na_2HPO_4, 2 mM NaH_2PO_4, and 1 mM Na_2EDTA, pH 7.2, containing 0 or 70% D_2O. The DNA concentration has been held constant and is 17.3 mM in base pairs. Spectra have been accumulated at 360 MHz by using a Redfield 214 pulse sequence (Redfield & Kunz, 1975); the total pulse time is 370 μs, with a 2628-Hz offset from water. A delay between pulses was used which was sufficiently long so that additional increases failed to increase resonance areas. Chemical shifts have been referenced to external Me_4Si. The temperature was held constant at 23 °C. (Top) 100% H_2O, 1000 transients. (Bottom) 30% H_2O, 1000 transients.

DNA as a wormlike flexing motion of the helix itself, rather than a fluctuation of nucleotide geometry inside the helix.

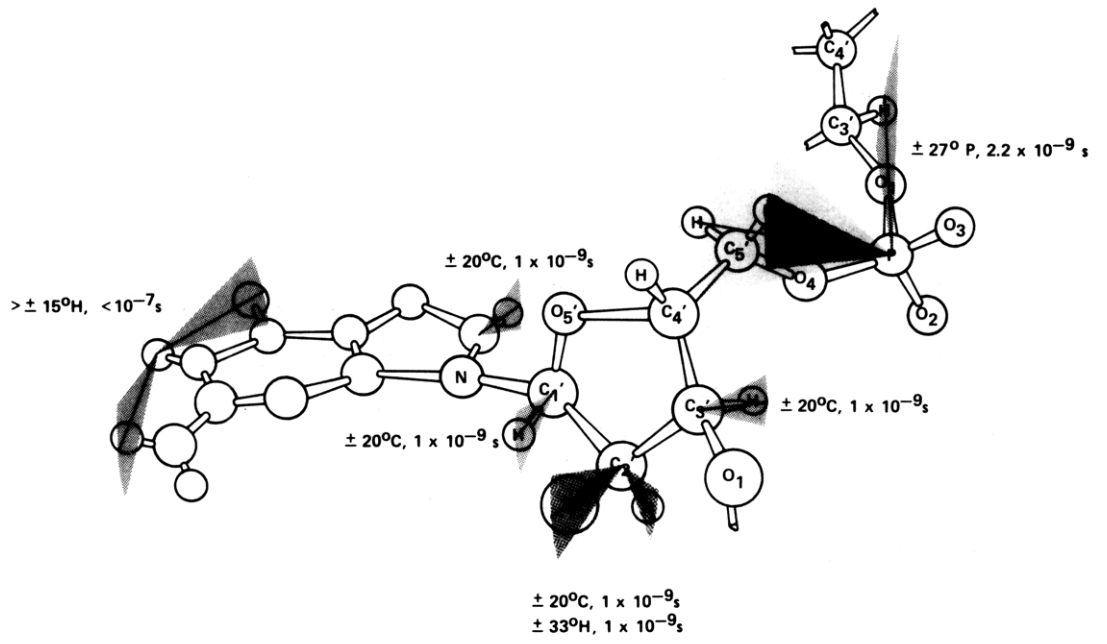

FIGURE 8: A map of DNA internal motions.

Literally interpreted, the Early model predicts that DNA behaves hydrodynamically as freely jointed segments 30–70 base pairs long. That prediction for DNA specifies a hydrodynamic persistence length which is very much shorter than the values measured for double-stranded DNA (Gray & Hearst, 1968). Moreover, that kind of wormlike flexing motion involves the cooperative motion of many DNA base pairs. We have shown elsewhere that the fast motion monitored by NMR may be stopped within a region as small as the two base pair long ethidium bromide binding site, leaving motion monitored in adjacent base pairs intact (Hogan & Jardetzky, 1980). So although the Early and Kearns calculations show convincingly that the DNA base planes experience an internal motion, those calculations may not be accurate in a quantitative sense.

In a B type helix (Arnott et al., 1969), the proton neighbors closest to the N(1) proton of a GC base pair are the two adjacent base-paired protons, 2.5 and 2.1 Å away. In an AT base pair the closest neighbor to $H_{N(3)}$ is the other base-paired proton at 2.4 Å and the adenine proton H_2 at 2.9 Å (Arnott et al., 1969). If N(1) and N(3) proton line widths are determined by dipolar interactions with adjacent H-bonded protons, then, when they are exchanged for deuterium, measured line widths should be greatly reduced. We calculate that, if exchangeable protons in DNA were substituted 70% with deuterium, then the dipolar contribution to GC proton line widths would decrease by 70% and AT base-pair line widths by 50%.

In Figure 7 is shown the spectrum of H-bonded AT and GC resonances after dialysis against a buffer containing 70% D_2O. As seen in Figure 7 and listed in Table V, measured line widths do not change although the resonance area is decreased by 70%. From this we conclude that H–H dipolar relaxation does not contribute significantly to the line widths of the N(1) and N(3) base-paired protons in 140 base pair long DNA. This is in contrast to the significant dipolar contribution which Early and Kearns have cited in Table I of their study. We can offer no explanation for this discrepancy. We do, however, note that the spectra which they have shown for a 154 base pair long fraction appear to change little in 66% D_2O (Early & Kearns, 1979).

If a 140 base pair long helix were rigid, the contribution of proton dipolar broadening to N(1) or N(3) proton resonances would be greater than 500 Hz (Hogan & Jardetzky, 1979). That contribution can be reduced only by motional narrowing. Therefore, as we concluded from ^{13}C relaxation measurements, a small contribution of proton–proton broadening to the measured line widths indicates, without assumption, that base planes experience fast motions in the helix. Although the details of that motion cannot be calculated from proton line widths alone, we calculate from the two-state model that for H–H dipolar relaxation to be as small as we or Early and Kearns have measured, H–H vectors must fluctuate by at least ±15° in 140 base pair long DNA with a time constant faster than 10^{-8} s.

Conclusions

From a combination of ^1H, ^{31}P, and ^{13}C NMR relaxation measurements on monodisperse DNA fragments, we have been able to calculate the rate and amplitude of DNA internal motions at several positions in the helix. A map of those motions is presented in Figure 8 superimposed on the canonical structure of B DNA (Arnott et al., 1969).

Motion is depicted as an arc directed toward the long helix axis, the extremes of the displacement corresponding to the values calculated from the two-state model. Motion may also occur perpendicular to Z, although it is expected to have a much smaller contribution to the relaxation properties of DNA. Therefore, the amplitudes which we have calculated here are approximately equal to the vertical projection of those fast motions which occur in the helix.

Several important conclusions from our calculations are summarized in Figure 8. First, ^1H and ^{13}C relaxation calculations of motion at position 2′ are in good agreement, both in terms of calculated amplitude and relaxation time. That agreement serves as an internal check for consistency. Second, we have shown that large motions occur at the base plane, at the deoxyribose sugar, and at the sugar–phosphate backbone which within a factor of 2 in rate appear to display the same internal correlation time. This correspondence cannot prove but is consistent with the idea that these motions are coupled to one another.

From kinetic data alone we cannot specify uniquely the conformational changes which give rise to the motions we have monitored. The range of possible models is, however, severely

limited by these kinetic measurements and by properties which are known of the B DNA helix. As we have shown, the internal motions not only are fast but also, as expected, have a small calculated activation energy; on the time average nearly every nucleotide in the helix experiences the motions, implying that the extremes of conformational change are nearly isoenergetic. Therefore, the possible internal motions cannot involve major changes in base stacking; the ΔH for unstacking a base pair (±20 kcal) is simply too unfavorable (Riesner & Römer, 1973). To be consistent with the known hydrodynamic properties of DNA, the motion cannot lead to a local bending of the helix greater than 4 or 5° (Barkley & Zimm, 1979). This precludes kinking as the origin of the internal motions (Crick & Klug, 1975).

For computational simplicity, we have modeled internal motion as a two-state isomerization, although multistate motions or continuous harmonic fluctuations about a single geometry could also fit the data. However, in the context of these models, amplitudes and calculated correlation times would change only to a small extent. Therefore, for the purposes of discussion, we describe here one type of simple two-state internal motion which could, in principle, account for the relaxation properties of DNA and for several of its other physical properties.

Levitt has recently proposed an alternative B DNA conformation which has a calculated energy as low as or lower than the DNA structure inferred from X-ray diffraction of solid samples (Levitt, 1978). In that altered conformation, the deoxyribose sugar assumes $O_{1'}$ endo rather than $C_{3'}$ endo sugar-pucker geometry; the base planes are propeller twisted approximately 20° from the perpendicular to the helix axis, and the geometry of the deoxyribose–phosphate backbone is substantially altered, giving rise to a 1.7° increase in the helical twist angle per base pair (Levitt, 1978). If this occurred with a time constant between 1×10^{-9} and 2×10^{-9} s, a local isomerization between a canonical B type geometry and an altered Levitt-type structure would give rise to deoxyribose, ribose–phosphate, and base-plane motions of the kind we have measured in DNA.

This kind of motion is also feasible from an energetic and from a structural perspective. Levitt has recently calculated that the canonical and the propeller twisted structure can coexist in a linear DNA helix (M. Levitt, personal communication). Therefore, as demanded by experiment, the proposed fast isomerization between these two structures is nearly isoenergetic and retains the linearity of the helix.

The proposed isomerization is also interesting in that it predicts that the twist angle between base pairs should fluctuate in DNA by about 2° with a rate near 10^{-9} s. Such fast twisting motions have in fact been measured recently by using electron spin resonance (ESR) (Robinson & Lerman, 1979) and fluorescent DNA labels (Genest & Wahl, 1978) and do appear to involve 2–4° fluctuations with a time constant $< 10^{-8}$ s.

This proposed isomerization also predicts that on the time average, the short axis of the base planes should be tipped substantially from the perpendicular to the long helix axis. By use of electric dichroism, it has recently been determined that in solution the short axis of the DNA bases is inclined at least 17–19° from the perpendicular (Hogan et al., 1978). When bound to DNA under similar experimental conditions, the drugs proflavin (Hogan et al., 1979a), 1-methylphenyl neutral red (Hogan et al., 1979a), and ethidium bromide (Hogan et al., 1979b) have one or more molecular axes which are measured by electric dichroism to be nearly perpendicular to the long helix axis. The ability to measure perpendicular drug orientation and twisted DNA orientation on the same DNA fragment confirms in a direct way the twisted base-plane geometry measured by electric dichroism.

In those studies it was assumed that this base-plane twist reflected a static DNA geometry. In light of DNA relaxation measurements, it is likely that the average 17° inclination of the bases arises as a very fast motional average.

References

Arnott, S., Dover, S. D., & Wonocott, A. J. (1969) *Acta Crystallogr., Sect. B B25*, 2192–2206.

Barkley, M. S., & Zimm, B. H. (1979) *J. Chem. Phys. 70*, 2991–3008.

Broersma, S. (1960) *J. Chem. Phys. 32*, 1626–1631.

Crick, F. H. C., & Klug, A. (1975) *Nature (London) 255*, 530–533.

Doddrell, D., Glushko, V., & Allerhand, A. (1972) *J. Chem. Phys. 56*, 3683–3689.

Dorman, D. E., & Roberts, J. D. (1970) *Proc. Natl. Acad. Sci. U.S.A. 65*, 19–26.

Early, T. A., & Kearns, D. R. (1979) *Proc. Natl. Acad. Sci. U.S.A. 76*, 4170–4174.

Genest, D., & Wahl, P. L. (1978) *Biophys. Chem. 7*, 317.

Gray, H. B., & Hearst, J. E. (1968) *J. Mol. Biol. 35*, 111–129.

Hogan, M. E., & Jardetzky, O. (1979) *Proc. Natl. Acad. Sci. U.S.A. 76*, 6341–6345.

Hogan, M. E., & Jardetzky, O. (1980) *Biochemistry 19*, 2079–2085.

Hogan, M. E., Dattagupta, N., & Crothers, D. M. (1978) *Proc. Natl. Acad. Sci. U.S.A. 75*, 195–199.

Hogan, M. E., Dattagupta, N., & Crothers, D. M. (1979a) *Biochemistry 18*, 280–288.

Hogan, M. E., Dattagupta, N., & Crothers, D. M. (1979b) *Nature (London) 278*, 521–524.

Jones, A. J., Winkley, M. W., Grant, D. M., & Robins, R. K. (1970) *Proc. Natl. Acad. Sci. U.S.A. 65*, 27–30.

Kalk, A., & Berendsen, H. J. C. (1976) *J. Magn. Reson. 24*, 343–366.

King, R., & Jardetzky, O. (1978) *Chem. Phys. Lett. 55*, 15–23.

King, R., Mass, R., Gassner, M., Nanda, R. K., Conover, W. W., & Jardetzky, O. (1978) *Biophys. J. 24*, 103–113.

Klevan, L., Armitage, I. M., & Crothers, D. M. (1979) *Nucleic Acids Res. 6*, 1607–1616.

Kovacic, R. T., & van Holde, K. E. (1977) *Biochemistry 16*, 1490–1498.

Lamb, H. (1945) in *Hydrodynamics*, Dover Publications, New York.

Levitt, M. (1978) *Proc. Natl. Acad. Sci. U.S.A. 75*, 640–644.

Redfield, A. G., & Kunz, S. D. (1975) *J. Magn. Reson. 19*, 114–117.

Riesner, R., & Römer, R. (1973) in *Physico-Chemical Properties of Nucleic Acids* (Duchesne, J., Ed.) Vol. 2, pp 237–319, Academic Press, New York.

Robinson, B. H., & Lerman, L. S. (1979) *Abstracts, Stereodynamics of Molecular Systems*, p 9, Buffalo, NY.

Sundaralingam, M. (1975) *Struct. Conform. Nucleic Acids Protein–Nucleic Acid Interact., Proc. Annu. Harry Steenbock Symp., 4th (1974)*, 487–529.

Woessner, E. D. (1962) *J. Chem. Phys. 37*, 647–654.